Supplementary information

Towards tunable graphene phononic crystals

Yuefeng Yu[1], Jan N. Kirchhof[1*], Aleksei Tsarapkin[2], Victor Deinhart[2,3], Oguzhan Yucel[1], Bianca Höfer[1], Katja Höflich[2] and Kirill I. Bolotin[1]*

[*]Authors contributed equally to this work.

[1]Department of Physics, Freie Universität Berlin, Arnimallee 14, 14195 Berlin, Germany.

[2]Ferdinand-Braun-Institut gGmbH Leibniz-Institut für Höchstfrequenztechnik, Gustav-Kirchhoff-Str. 4, 12489 Berlin, Germany.

[3]Helmholtz-Zentrum Berlin für Materialien und Energie, Hahn-Meitner-Platz 1, 14109 Berlin, Germany.

Keywords: Nanomechanics, phononic crystal, graphene, optomechanics, resonators, NEMS

I. Sample fabrication

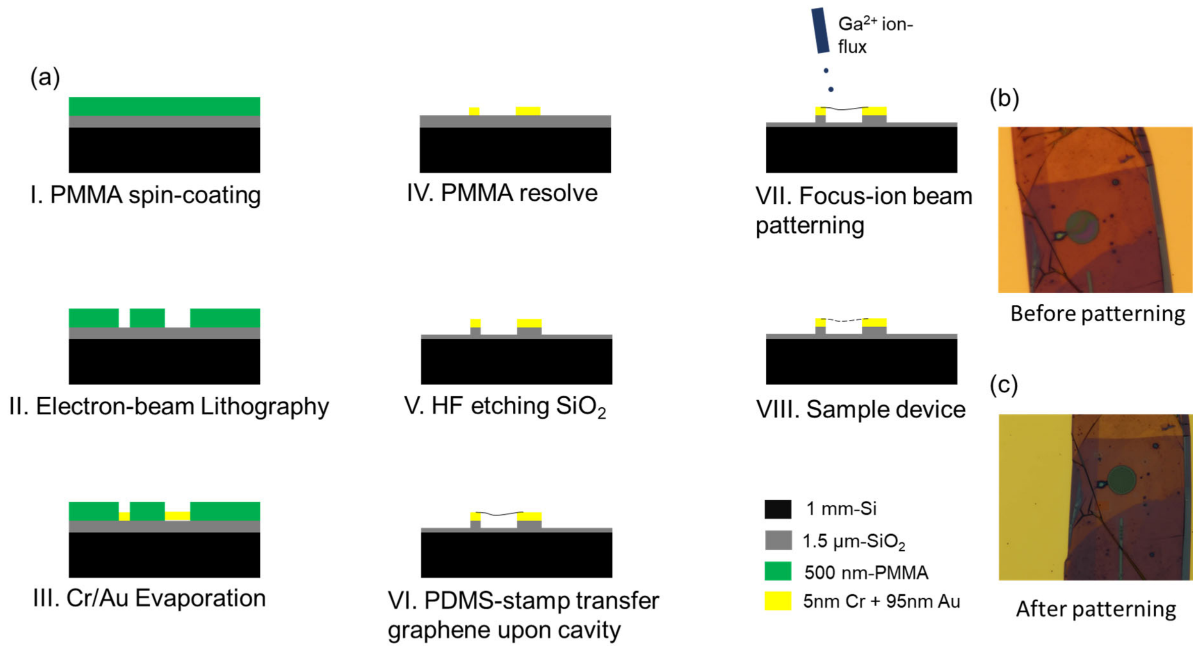

Fig. S1: Procedure of sample fabrication *a) fabrication of substrate chip and device. b) SEM image before b) and after c) FIB patterning*

Device are fabricated starting with Si/SiO2 wafer pieces (0.5 cm*0.5 cm width/length; thickness of SiO2 is 1.5um). The procedure of substrate fabrication is shown in Fig. S1. In step III, 5nm Cr/95nm Au is evaporated. In step V, about 1060nm of the SiO2 layer is etched leaving the rest of the oxide as an insulating layer. Such a depth enables strong interferometric signal ($g_0 = (2N+1)\cdot\frac{\lambda}{4}$, N is positive integer and rest of parameters are explained in section II, III) and a large deflection of the membrane center and therefore large strain. In step VI, graphene is transferred onto the cavity. At this point, large variations in membrane's thickness are observed (red regions of the membrane seen in Fig. S1b). These variations disappear after FIB patterning of the membrane (step VIII).

II. Sensitivity calibration under IF bandwidth of 10 Hz

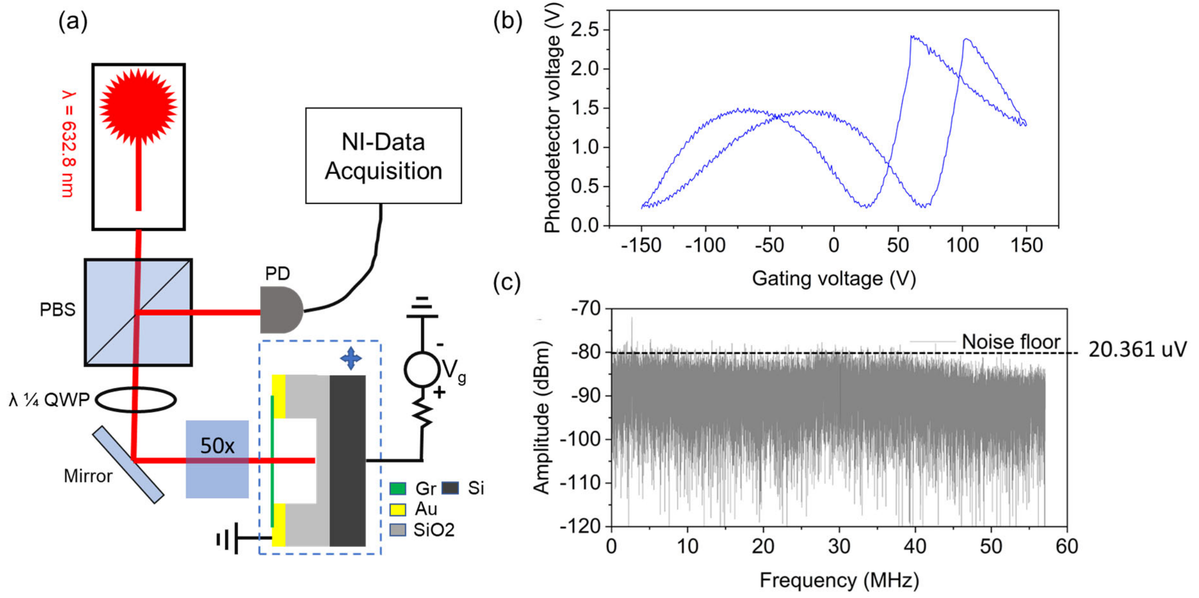

Fig. S2: Characterization of measurement sensitivity *a) Experimental setup b) Voltage on a photodetector vs. gating voltage. Lowest reflection is seen when the signal on photodetector is* V_{min}*=0.235 V, the highest signal is* V_{max}*=2.414 V. c) Noise floor spectrum measured by disabling electrical actuation.*

Our goal is to quantitatively determine the amplitude of mechanical vibration of the membrane. To do this, we need to convert the signal recorded by the photodetector (PD) in the units of Volt into displacements in the unit of meter [1,2]. In Fig. S2b, we show the PD signal (V_{PD}) vs. the gate voltage. The periodic variation of the amplitude corresponds to the membrane moving across the standing-wave pattern inside the cavity. We can analytically estimate the signal on the photodetector assuming it is proportional to the light intensity reflected from the cavity containing graphene:

$$I_{tot} \propto \mathrm{const}(P_{in}) + \cos\left(\varphi_{gr}(z) - \varphi_0\right) \quad (1)$$

Here $\varphi_{gr} = \frac{2\pi}{\lambda} \cdot 2z$ is the phase acquired by the light wave on the travel across the cavity, and φ_0 is a phase shift dependent on the SiO_2 thickness, which can be defined as reference phase shift, $\varphi_0 = 0$. P_{in} is the incident laser power, determining the constant term in eq.S1. We see that the light intensity goes from a minimum to a maximum when the membrane is moved by the distance $z = \frac{\lambda}{4}$. Experimentally, we see that a minimum and a maximum of intensity correspond to the photodiode voltages $V_{min} = 0.235\ V$ to $V_{max} = 2.414\ V$. Assuming that for most of our experiments the membrane is located between the maximum and a minimum, we can therefore determine the amplitude of a vibration of the membrane z_{ac} to the amplitude of the signal of on the photodetector $\widetilde{V_{ac}}$ using linear interpolation:

$$z_{ac} = \frac{V_{max} - V_{min}}{\widetilde{V_{ac}} \cdot {}^{\lambda}/_{4}} \quad (2)$$

Finally, we can obtain the amplitude of noise in our system. We disable electrical actuation by grounding the sample and record a spectral noise amplitude (Fig. S2c). From the noise floor of the measurement, around -80 dBm, we estimate the sensitivity of the measurement into a 10Hz IF bandwidth:

$$s = \frac{\widetilde{V_{ac}}}{\frac{V_{top} - V_{bot}}{\lambda/4} * \sqrt{IF}} < 0.5\ \mathrm{pm}/\sqrt{Hz} \quad (3)$$

III. Built-in tension and membrane density

The goal of this section is to estimate the built-in tension as well the density of the membrane from experimental data. In general, the resonance frequency of a suspended circular membrane in a field effect transistor geometry, with voltage V applied between the membrane is the gate below is evaluated in Ref. [3]:

$$f^2(V) = \frac{1}{4m\pi^2}\left[\frac{2\pi Eh\epsilon}{1-v^2} + \frac{(1-v)\pi\varepsilon_0^2 r^2}{8(1+v)Eh\epsilon^2 g_0^4}V^4 - \frac{0.542\varepsilon_0\pi r^2}{2g_0^3}V^2\right] \quad (4)$$

where m is the effective mass, ϵ is built-in strain, E is Young's modulus of a suspended membrane after patterning, h = 10^{-9} m is its effective thickness, $v = 0.15$ is the Poisson ratio, r = $9.9*10^{-6}$ is radius of the suspended region, g_0 = $1.206*10^{-6}$ m is the effective separation between membrane's center and the bottom gate. The effective separation is defined as $g_0 + \frac{t_{SiO_2}}{\varepsilon_{SiO_2}}$, where g is the membrane/SiO_2 distance and t_{SiO_2} – thickness of SiO_2. Treating $E\epsilon$ and m as free parameters we fit the experimental data in the region V< 66 V.

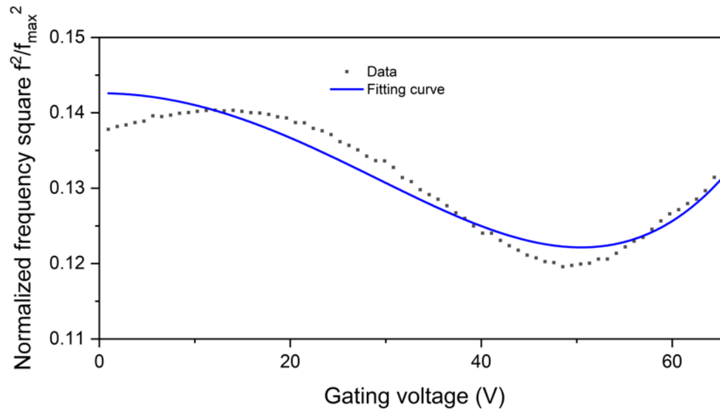

Fig.S3: fundamental-vibrational-mode frequency response from gating voltage

From the fit, we obtain $E\epsilon = 436\,MPa$, effective mass $m = 1.06 * 10^{-14}\,kg$. Area of patterned membrane $A = \pi r^2 - N\pi r_h^2$, where r_h = is the radium of single hole in pattern, N = 270 is the total number of cut holes in the pattern. Converting, we obtain $\rho_{2D} = \frac{m}{A} = 5.2 \times 10^{-5} kg/m^2$, built-in tension is $T_{built-in} = E\epsilon h = 0.44\ N/m$.

We note that our fitting only works in the regime of small gate voltage, the region of so-called capacitive softening [3–5]. At large gate voltage, we see that the fit does not describe the data well. We hypothesize that this is related to the buckling transition in our patterned membrane.

IV. Midgap modes inside the phononic bandgap

Our experiments suggest that there are modes localized withing the region of a phononic bandgap at high strain. In Fig. S4, we demonstrate that such modes appear in a simulation accounting for boundary condition and finite device size.

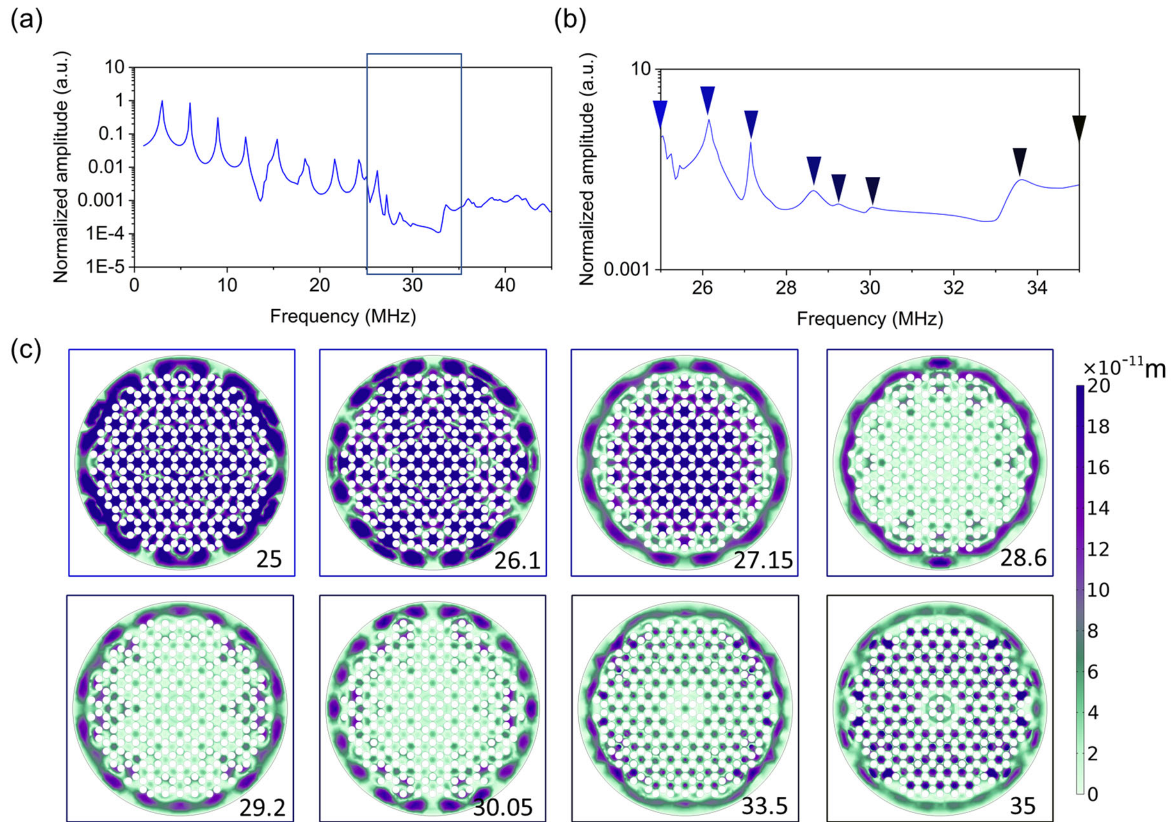

Fig. S4: Midgap modes in a finite-size phononic crystal *(a) Resonance spectrum, same as in Fig.1f. (b) Zoom-in of the bandgap region 25–35MHz showing a number of modes inside the bandgap region (c) Spatial distribution of the amplitude of several of the modes visible in (b) (The frequency of each mode in MHz is shown in the bottom right corner). All of the modes are localized at the edge of the membrane and do not appear in "infinite" simulations neglecting finite device size.*

V. Comparing patterned and unpatterned devices

To confirm that the observed phononic bandgap originate from a pattern of holes cut in our device, we fabricated, measured and simulated a graphene device without patterning. We only detect first 4 modes in such a device and no signature of a bandgap (Fig. S5a). Likewise, COMSOL simulation of phononic spectrum of the unpatterned device exhibit multiple vibrational modes with roughly constant mode density without any signature of a bandgap region (Fig. S5b).

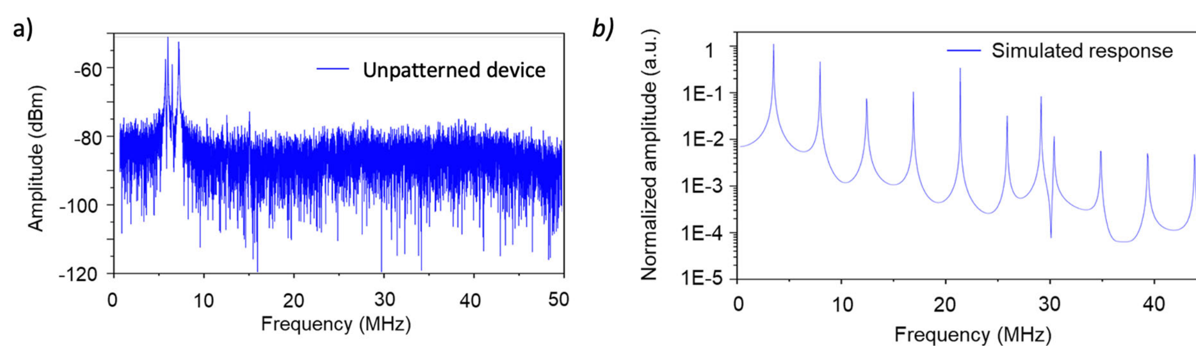

Fig. S5: Vibration of graphene drum head w/o pattern. *(a) Resonance response spectrum of an unpatterned graphene drum under strong drive of 8 dBm. (b) Simulated response of (a).*

Reference

1. Callera Aguila, M. A. *et al.* Fabry-Perot interferometric calibration of van der Waals material-based nanomechanical resonators. *Nanoscale Adv.* **4**, 502–509 (2022).
2. Esmenda, J. C. *et al.* Optoelectrical Nanomechanical Resonators Made from Multilayered Two-Dimensional Materials. *ACS Appl. Nano Mater.* **5**, 8875–8882 (2022).
3. Chen, C. Graphene NanoElectroMechanical Resonators and Oscillators. *Thesis Columbia* (2013).
4. Weber, P., Güttinger, J., Tsioutsios, I., Chang, D. E. & Bachtold, A. Coupling graphene mechanical resonators to superconducting microwave cavities. *Nano Lett.* **14**, 2854–

2860 (2014).

5. Šiškins, M. *et al.* Nanomechanical probing and strain tuning of the Curie temperature in suspended Cr2Ge2Te6-based heterostructures. *npj 2D Mater. Appl.* **6**, 1–8 (2022).